ChemComm

COMMUNICATION

View Article Online
View Journal | View Issue

Cite this: *Chem. Commun.*, 2018, **54**, 814

Received 11th September 2017,
Accepted 2nd January 2018

DOI: 10.1039/c7cc07082a

rsc.li/chemcomm

Breathing and oscillating growth of solid-electrolyte-interphase upon electrochemical cycling†

Zengqing Zhuo,[ab] Peng Lu,[c] Charles Delacourt,[d] Ruimin Qiao,[b] Kang Xu,[e] Feng Pan,*[a] Stephen J. Harris*[f] and Wanli Yang*[b]

We report the first direct experimental evidence of the dynamic behavior of the solid-electrolyte-interphase (SEI) on copper electrodes upon electrochemical cycling. Synchrotron-based soft X-ray absorption spectroscopy (sXAS) and time-of-flight secondary ion mass spectrometry (TOF-SIMS) consistently show that both the chemical composition and the thickness of the SEI change with electrochemical potential throughout the slow formation process. In particular, sXAS results show that the nascent carbonate species in SEI show redox reversibility and decompose during the delithiation (oxidation) process, which leads to a significant shrinking of the SEI thickness as confirmed by TOF-SIMS. Meanwhile, the carbonates also matures and become more and more inactive at every lithiation (reduction) process. These experimental observations reveal unambiguously that SEI formation is much more complicated than a simple and monotonous deposition of electrolyte decomposition product; instead, it could be an oscillating process with a breathing growth.

Lithium ion batteries (LIBs) have been ubiquitous in modern society. However, both fundamental understanding and practical developments are required in order to advance battery technology to the next level in both the performance and stability.[1] In the history of the battery development, it has long been noticed that an elusive solid-electrolyte-interphase (SEI), formed on the electrode surfaces in battery due to the sacrificial decomposition of electrolyte components, plays a critical role in stabilizing the electrochemical operation far from their thermodynamic equilibria.[2] SEI forms on the surface of the lithiated negative electrode (anode) in the initial cycles, and the process, although consuming electrolyte and lithium, leads to kinetic protection against further decomposition of electrolyte (blocking electron transport) while still allowing Li^+-diffusion. Fundamentally, the understanding of the SEI has greatly advanced over the last two decades, especially on graphite anode surfaces.[3] By conventional wisdom, a SEI in LIBs is typically considered "stable" once formed, and its quality and chemistry could be manipulated with various additives,[2,4,5] or surface modification of electrodes.[6] Despite the well-recognized "stability", SEI is also known to evolve slowly in the LIBs upon extended electrochemical cycling until its mechanical and/or electronic failure, which often means the end of the battery life.[7] Onerous efforts[2,5,8–12] have been made to understand the formation process of SEI through various techniques such as Raman spectroscopy, XPS, FTIR, AFM, SEM, and *in situ* TEM *et al.*[9,12–14] Correlation between anode SEI chemistry and Li^+-solvation structure was established.[2,3,5] However, the mechanism, design and control of SEI remain elusive and a formidable challenge for LIBs.[10] In particular, studies of the live-formation and evolution of SEI upon electrochemical cycling has been limited to mostly macroscopic and phenomenological tools like impedance.[8,15] Whether a formed SEI is truly stable, as expected in conventional wisdom, or changes upon electrochemical cycling remains to be explored with the help of elemental and chemically sensitive probes.

In this work, we deliberately formed a model SEI layer on Cu surface and monitored its chemical and mechanical responses to electrochemical potentials. Cu is selected because of its inertness toward reduction, and it provides an ideal template for SEI growth free of the interference from insertion process that would otherwise take place for other electrodes like graphite.[8,16,17] Our sXAS and TOF-SIMS results provide direct evidence of strong SEI variations upon electrochemical states, in both chemical and mechanical properties. The carbonates are largely responsible for the constant evolution of the SEI through its decomposition, which causes a significant decrease of the SEI thickness in the delithiated state. In the meantime, the carbonates keep forming during each lithiation process,

[a] *School of Advanced Materials, Peking University, Shenzhen Graduate School, Shenzhen 518055, China. E-mail: panfeng@pkusz.edu.cn*
[b] *Advanced Light Source, Lawrence Berkeley National Laboratory, Berkeley, CA 94720, USA. E-mail: wlyang@lbl.gov*
[c] *General Motors Research and Development Center, Warren MI 48090, USA*
[d] *Laboratoire de Réactivité et de Chimie des Solides, CNRS UMR 7314, Université de Picardie Jules Verne, Amiens, France*
[e] *Electrochemistry Branch, Sensor and Electron Devices Directorate Power and Energy Division U.S. Army Research Laboratory, Adelphi, MD 20783, USA*
[f] *Materials Science Division, Lawrence Berkeley National Laboratory, Berkeley, CA 94720, USA. E-mail: sjharris@lbl.gov*

† Electronic supplementary information (ESI) available. See DOI: 10.1039/c7cc07082a

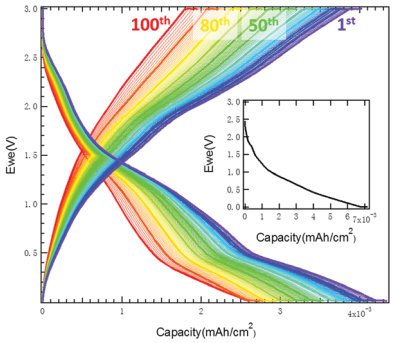

Fig. 1 The galvanostatic charging curve of the SEI formation (inset) and further cycling of a Cu electrode in electrolyte 1 M $LiClO_4$, EC : DEC (1 : 1 by wt). The overstriking lines indicate the profile of the 1, 10, 20, 100 cycles.

and experience an apparent maturing process by becoming less and less electro-chemically active as the number of cycles increases.

A model SEI is formed and cycled on the surface of a well-polished Cu electrode. The experimental setup has been reported in a previous work, and more details on the electrochemical cell is provided in the Fig. S1 of the ESI.†[17] The technical details on sXAS and TOF-SIMS are provided in the ESI.† The SEI is formed at the constant current (15 μA cm^{-2}) until the potential reaches the cutoff value (0.005 V); then the voltage is held constant. This process simulates the SEI formation in actual LIB, whose anode is subject to gradual cathodic polarization and offers opportunity for the selective reduction of electrolyte components. Fig. 1 (inset) shows that the formation capacity is about 6.7 μA h cm^{-2}, with the potential decay for less than 30 min. The formed SEI is then cycled galvanostatically in the same electrochemical cell between 0.005 and 3 V. The galvanostatic charging curve up to 100 cycles is displayed in Fig. 1, and magnified in Fig. S2 (ESI†). The cycling capacities decay quickly, indicating that the surface is gradually passivated; however, the SEI obviously remains electrochemically active over 100 cycles that is beyond what chemical dissolution effect could account for.[18] We cannot completely rule out the contribution from the electrochemical reduction of a thin copper oxide layer covering the copper electrode, *i.e.*, $Cu_xO + 2Li^+ + 2e^- \leftrightarrows xCu + Li_2O$.[19] Also, as reported for CoO electrodes before,[20] the surface oxide may facilitate the decomposition reaction of the SEI, which likely lengthens the SEI stabilization process as observed here. The possible surface reaction is not the focus of this study, and here we concentrate on the activities of the SEI signal itself, which are well separated from any (O) signals from the surface Cu_xO.

Fig. 2 shows the C K-edge sXAS results of a series of SEI samples at different cycling stages, collected at BL 8.0.1 of the ALS.[21] The full C K-edge sXAS results are in Fig. S3 (ESI†). sXAS is a spectroscopic technique with inherent elemental and chemical sensitivity, as well as two different probe depths of about 10 and 100 nm through total electron yield (TEY) and total fluorescence yield (TFY) modes, respectively.[22] It has been successfully utilized to gain insights into the chemical composition of SEIs.[17,23,24] For all five samples, three distinct features could be found at 285 eV, 288.6 eV, and 290.2 eV. The 285 eV feature can be attributed to C=C π* bonds. The 288.6 eV feature is from the C–H σ-bonds of $–CH_2–$ and $–CH_3$.[25] The most striking absorption feature, at 290.2 eV, originates from the electron dipole transition between C 1s core level and the π*(C=O) orbital of the carbonate (CO_3^{2-}) functional group.[25,26] The assignment of the main features could be directly seen through the comparison with the spectra from two reference standards lithium ethylene dicarbonate (LEDC) and lithium acetate ($H_3C–COO–Li$), which are plotted at the bottom of Fig. 2. It could be seen that the overall lineshape of the SEI sXAS is dominated by the 290.2 (CO_3^{2-}) and 288.6 ($–CH_2–COO–$) eV features, indicating large amount of carbonyl species, such as semi-carbonate, oxalate or carboxylate, as expected for SEIs formed through EC:DEC electrolyte.

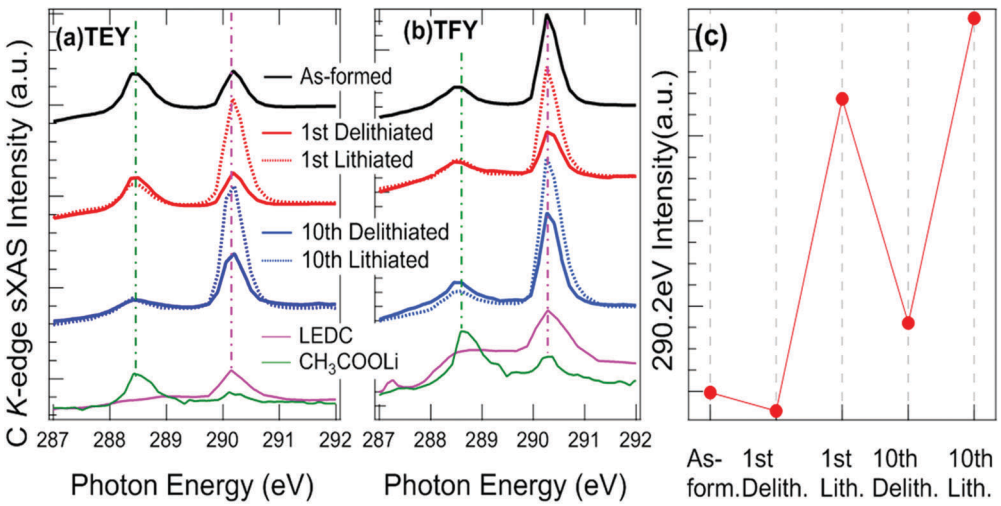

Fig. 2 (a) C K-edge TEY spectra of the as-formed SEI (black), and the SEIs at delithiated (solid lines) and lithiated (dotted lines) states at the 1st (red) and 10th (blue) cycles. (b) C K-edge TFY spectra of the same series of SEIs. (c) The intensity evolution of the carbonate C-K TEY feature at 290.2 eV upon electrochemical states.

More importantly, Fig. 2 displays a strong evolution of the sXAS lineshape upon electrochemical cycling. In particular, the 290.2 eV carbonate peak intensity is greatly enhanced at the lithiated states, but decreases significantly at the delithiated states. Furthermore, the overall amount of carbonates keeps increasing upon cycling; *e.g.*, the 290.2 eV peak intensity after 10 cycles is much stronger compared with that of the 1st cycle SEI. The observation of the contrasting carbonate signal in the delithiated/lithiated states is the same in both the TEY and TFY modes, indicating that this is an overall change on the chemical composition throughout the SEI layer.

In Fig. 2c, we display the TEY intensity evolution of the 290.2 eV carbonate feature at different electrochemical states. The absolute intensity of TFY suffers self-absorption effect, so only TEY data are used for this quantitative analysis. Two trends of carbonate evolution can be clearly identified. (i) In general, carbonate species are formed during lithiation (when the SEI is held at low voltage), but are re-oxidized during delithiation (when voltage is raised). The carbonate decomposition in SEI has been reported in theory by Leung *et al.*,[27] but the quantitative difference on the potential range is likely due to the different electrodes. (ii) Not all the formed carbonate participates this re-oxidization in the electrochemical cycling; therefore, the overall amount of carbonate keeps increasing with cycling. This is also consistent with the electrochemical profile, which shows higher lithiated capacity than delithiated capacity at each cycle (Fig. 1 and Fig. S2, ESI†). Thus, the SEI formation is a slow evolution process on Cu electrodes. With more and more carbonates formed and becoming inert against re-oxidation, the SEI will eventually become an ideal passivating layer with a large amount of carbonates.

The evolution of the SEI is further confirmed by O K-edge sXAS results, as shown in Fig. 3, with full spectra in Fig. S4 (ESI†). The feature at 533.7 eV can be attributed to O1s → π* transitions (C 2p–O 2p derived orbitals), which is a characteristic peak of the carbonate (CO_3^{2-}) function group.[26] The shoulder feature at 532.4 eV is from organic compounds like oxalate and/or OH function groups, which can be directly seen through the comparison with the reference spectra in Fig. 3. Again, the carbonate feature at 533.7 eV is enhanced in the lithiated state, while partially suppressed in the delithiated state. The evolution of the carbonate-feature intensity is summarized in Fig. 3c, which shows the same breathing behavior as that from C-K sXAS results, indicating the nascent carbonate is partially oxidizable during electrochemical operation and continues to form for extended cycles in such system.

In addition to sXAS, we also performed TOF-SIMS experiments in order to better understand the morphology and general chemical composition. Fig. 4 shows the TOF-SIMS profiles up to 100 nm depth of the SEIs at as-formed, 1st delithiated, and 1st lithiated states. The normalized intensity of three representative species are shown as $^6Li^+$, CH_2OLi^+, and Cu^+. $^6Li^+$ comes from all the lithium compounds, including the organic species and inorganic lithium salts, which include the signal from lithium containing carbonate species such as Li_2CO_3, LEDC *etc.* The CH_2OLi^+ represents lithium alkoxide or similar type of lithium species. The point where the $^6Li^+$ intensity drops to 1/2 of its initial value is consistent with the Cu^+ rising to about half of its ultimate intensity, which defines the SEI/Cu interface and taken as the thickness indicator (shadow in Fig. 4). Several important pieces of information are revealed here. First, the two indicators consistently mark the SEI thickness as 45, 10, and 60 nm for the as-formed, 1st cycle delithiated, and 1st cycle lithiated samples. This is consistent with the sXAS observation that the SEI grows in an oscillating pattern with electrochemical cycling. Second, the greatly reduced SEI thickness in the delithiated state corresponds to a relatively higher concentration of CH_2OLi^+ compared with other Li containing species. This might be caused by the carbonate re-oxidation that leads to low abundances in the delithiated state. For unclear reasons, the re-oxidation of alkoxide, if happens, proceeds at much slower rate than carbonates. Nevertheless, it is striking to see that SEI thickness shrinks so much in the delithiated state due to disappearance of carbonate species. Third, the TOF-SIMS data show that for the SEI at the lithiated states, the overall $^6Li^+$ and CH_2OLi^+ concentrations are more or less uniform across most of the SEI thickness.

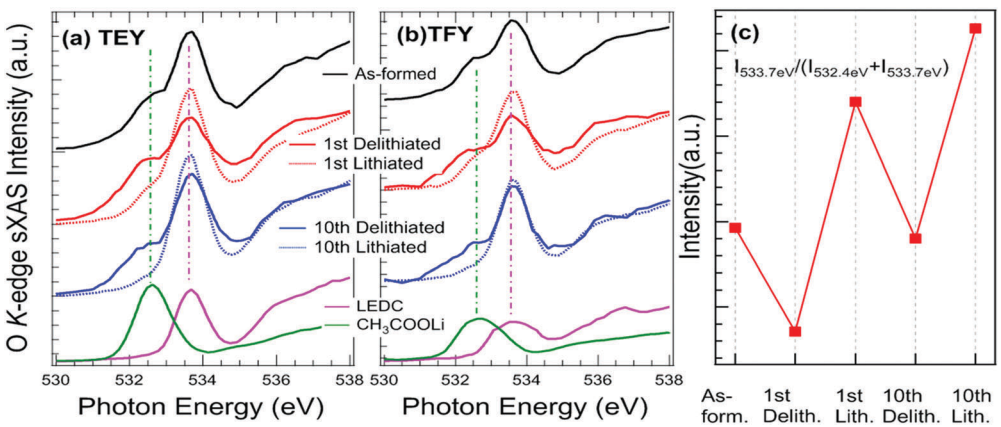

Fig. 3 (a) O-K TEY spectra of the as-formed SEI (black), and the SEIs at delithiated (solid lines) and lithiated (dotted lines) states at the 1st (red) and 10th (blue) cycles. (b) O K-edge TFY spectra of the same series of SEIs. (c) The intensity evolution of the O-K TEY feature at 533.7 eV upon electrochemical states.

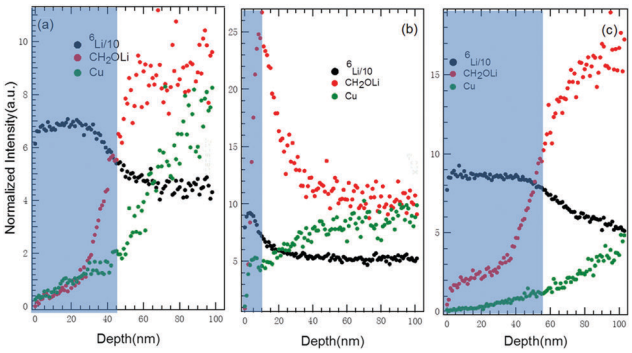

Fig. 4 The TOF-SIMS 100 nm depth profiles of the (a) as-formed SEI, (b) SEI at the 1st delithiated state, and (c) SEI at the 1st lithiated state, which are prepared in sequence. The $^6Li^+$ stands for all the lithium compounds, and its Intensity is scaled down by 10 times for display purpose. The CH_2OLi^+ represents the lithium alkoxide or similar type of lithium species. The shadows represent the thickness, about 45, 10, 60 nm, of the SEIs determined by both the Cu and $^6Li^+$ edges.

Therefore, the TOF-SIMS results are in excellent agreement with the sXAS analysis, showing that the re-oxidation of carbonates dramatically diminishes the overall SEI thickness in the delithiated state, while the SEI keeps growing through the lithiation process.

In summary, through a combination of soft X-ray spectroscopy and TOF-SIMS, we reveal that the SEI formation on a copper electrode is a highly dynamic process. The absence of the intercalation process on Cu electrodes provides an ideal template to study the intrinsic nature of SEI. The nascent carbonates in SEI are largely susceptible to re-oxidation during electrochemical cycling over extended cycles in this model system. The decomposition of carbonates in SEI during the delithiation significantly shrinks the thickness of the SEI layer. The carbonates in the SEI continue to form during each lithiation cycle, and gradually lose the electrochemical activity upon cycling. Our work provides unambiguous experimental evidence for an oscillating pattern of a slow SEI formation on Cu electrodes. We note that SEI formation on different electrodes is likely different in the pace and scale of its electrochemical activity, and detailed reaction mechanism requires further studies. Nonetheless, this work revises the conventional wisdom that SEI, once formed, is stable over long periods. It suggests that the SEI formation is far more complicated than simple accumulation of electrolyte decomposition products on electrode surface.

Advanced Light Source is supported by the Director, Office of Science, Office of Basic Energy Sciences, of the U.S. Department of Energy under Contract No. DE-AC02-05CH11231. This work was supported by Guangdong Innovation Team Project (No. 2013N080) and Shenzhen Science and Technology Research Grant (peacock plan KYPT20141016105435850).

Conflicts of interest

There are no conflicts to declare.

References

1 M. Armand and J. M. Tarascon, *Nature*, 2008, **451**, 652–657.
2 K. Xu, *Chem. Rev.*, 2004, **104**, 4303–4418.
3 K. Xu and A. von Wald Cresce, *J. Mater. Res.*, 2012, **27**, 2327–2341.
4 S. S. Zhang, *J. Power Sources*, 2006, **162**, 1379–1394.
5 K. Xu, *Chem. Rev.*, 2014, **114**, 11503–11618.
6 E. Peled and S. Menkin, *J. Electrochem. Soc.*, 2017, **164**, A1703–A1719.
7 M. B. Pinson and M. Z. Bazant, *J. Electrochem. Soc.*, 2013, **160**, A243–A250.
8 P. Lu, C. Li, E. W. Schneider and S. J. Harris, *J. Phys. Chem. C*, 2014, **118**, 896–903.
9 P. Verma, P. Maire and P. Novák, *Electrochim. Acta*, 2010, **55**, 6332–6341.
10 W. Martin, *Z. Phys. Chem.*, 2009, **223**, 1395–1406.
11 D. Aurbach, B. Markovsky, G. Salitra, E. Markevich, Y. Talyossef, M. Koltypin, L. Nazar, B. Ellis and D. Kovacheva, *J. Power Sources*, 2007, **165**, 491–499.
12 P. Abellan, B. L. Mehdi, L. R. Parent, M. Gu, C. Park, W. Xu, Y. Zhang, I. Arslan, J. G. Zhang, C. M. Wang, J. E. Evans and N. D. Browning, *Nano Lett.*, 2014, **14**, 1293–1299.
13 J. E. Owejan, J. P. Owejan, S. C. DeCaluwe and J. A. Dura, *Chem. Mater.*, 2012, **24**, 2133–2140.
14 H. Bülter, F. Peters, J. Schwenzel and G. Wittstock, *Angew. Chem., Int. Ed.*, 2014, **53**, 10531–10535.
15 D. Juarez-Robles, C.-F. Chen, Y. Barsukov and P. P. Mukherjee, *J. Electrochem. Soc.*, 2017, **164**, A837–A847.
16 P. Lu and S. J. Harris, *Electrochem. Commun.*, 2011, **13**, 1035–1037.
17 C. Delacourt, A. Kwong, X. Liu, R. Qiao, W. L. Yang, P. Lu, S. J. Harris and V. Srinivasan, *J. Electrochem. Soc.*, 2013, **160**, A1099–A1107.
18 K. Tasaki, A. Goldberg, J.-J. Lian, M. Walker, A. Timmons and S. J. Harris, *J. Electrochem. Soc.*, 2009, **156**, A1019–A1027.
19 S. Grugeon, S. Laruelle, R. Herrera-Urbina, L. Dupont, P. Poizot and J.-M. Tarascon, *J. Electrochem. Soc.*, 2001, **148**, A285–A292.
20 S. Laruelle, S. Grugeon, P. Poizot, M. Dolle, L. Dupont and J. M. Tarascon, *J. Electrochem. Soc.*, 2002, **149**, A627.
21 R. Qiao, Q. Li, Z. Zhuo, S. Sallis, O. Fuchs, M. Blum, L. Weinhardt, C. Heske, J. Pepper, M. Jones, A. Brown, A. Spucces, K. Chow, B. Smith, P.-A. Glans, Y. Chen, S. Yan, F. Pan, L. F. J. Piper, J. Denlinger, J. Guo, Z. Hussain, Y.-D. Chuang and W. Yang, *Rev. Sci. Instrum.*, 2017, **88**, 033106.
22 W. Yang, X. Liu, R. Qiao, P. Olalde-Velasco, J. D. Spear, L. Roseguo, J. X. Pepper, Y.-D. Chuang, J. D. Denlinger and Z. Hussain, *J. Electron Spectrosc. Relat. Phenom.*, 2013, **190**(part A), 64–74.
23 R. Qiao, I. T. Lucas, A. Karim, J. Syzdek, X. Liu, W. Chen, K. Persson, R. Kostecki and W. Yang, *Adv. Mater. Interfaces*, 2014, **1**, 1300115.
24 M. Balasubramanian, H. S. Lee, X. Sun, X. Q. Yang, A. R. Moodenbaugh, J. McBreen, D. A. Fischer and Z. Fu, *Electrochem. Solid-State Lett.*, 2002, **5**, A22–A25.
25 A. Augustsson, M. Herstedt, J. H. Guo, K. Edstrom, G. V. Zhuang, J. P. N. Ross, J. E. Rubensson and J. Nordgren, *Phys. Chem. Chem. Phys.*, 2004, **6**, 4185.
26 R. Qiao, Y.-D. Chuang, S. Yan and W. Yang, *PLoS One*, 2012, **7**, e49182.
27 K. Leung, F. Soto, K. Hankins, P. B. Balbuena and K. L. Harrison, *J. Phys. Chem. C*, 2016, **120**, 6302–6313.